Inkjet printed microfluidic paper-based analytical device (µPAD) for glucose colorimetric detection in artificial urine

Han Zhang[1] · Ethan Smith[2] · Wei Zhang[1] · Anhong Zhou[1]

Abstract

This article introduces a novel inkjet printing method for the fabrication of a microfluidic paper-based analytical device (µPADs) with improved analytical performance for colorimetric measurements. Firstly, a hydrophobic boundary was created by wax printing on chromatography paper. Then, chitosan (CHI), 3,3′,5,5′-Tetramethylbenzidine (TMB) and enzymatic mixture solvent (glucose oxidase (GOx) and horseradish peroxidase (HRP)) were sequentially printed in the sensing zone. Polyethylene glycol (PEG6000) was mixed with the bienzymatic solution to act as an enzyme stabilizer, forming the printable ink. The resulting µPADs exhibited a linear relationship between color intensity and glucose concentration from 0.0 25 mg/ml to 0 .5mg/ml. The detectable glucose concentration was in a clinically relevant range from 0.01 mg/ml to 4 mg/ml. The limit of detection (LOD) was achieved at 0.01 mg/ml. After 60-day storage under 4 °C, the color intensity at the testing zone retained over 80% of the original intensity. In addition, a smartphone application was developed for *in situ* colorimetric image processing, and the colorimetric analysis results were compared with those from the use of a scanner followed by processing using ImageJ. Furthermore, the development of this ink printing method also provides a point of care (POC) platform for other substances detection purposes.

Keywords µPAD · Colorimetric detection · Glucose · Inkjet printing · Smartphone-based assay

1 Introduction

Microfluidic paper-based analytical devices (µPADs) present unique opportunities in the development of rapid point-of-care tests (POCTs). Multiple conventional detection techniques, such as colorimetric detection, electrochemical detection, fluorescence, and Surface-enhanced Raman Spectroscopy have been integrated into paper-based devices for rapid POCTs (De Tarso Garcia et al. 2014; Dungchai et al. 2009; Evans et al. 2014b; Lee et al. 2010; Li et al. 2013, 2016; Liu and Crooks 2011; Määttänen et al. 2013; Thom et al. 2014; Wei and White 2013; Wei et al. 2016; Zhou et al. 2014). Due to its global affordability, user-friendliness, portability, and rapid visual readout (Martinez

✉ Anhong Zhou
  Anhong.Zhou@usu.edu

[1] Department of Biological Engineering, Utah State University, 4105 Old Main Hill, Logan, UT 84322-4105, USA

[2] Thayer School of Engineering, Dartmouth College, Hanover, NH 03755, USA

et al. 2009), colorimetric detection could be a very useful technique when coupled with µPADs. The color intensity can be measured by taking a photograph of the sensing zone on the µPADs using a scanner (Hu et al. 2014) or smartphone (Hu et al. 2014; Shen et al. 2012; Vashist et al. 2014).

In colorimetric glucose detection, glucose oxidase (GOx) and horseradish peroxidase (HRP) form a common enzyme pair used to catalyze the reaction between glucose and the chromogenic substrates (Evans et al. 2014a; Figueredo et al. 2015; Gabriel et al. 2016, 2017). The GOx firstly oxidizes glucose to gluconic acid and hydrogen peroxide (H_2O_2). Then, HRP catalyzes the reaction of H_2O_2 with chromogenic substrates and exhibits a blue color. The commonly used chromogenic substrates for HRP include KI, TMB, DAB, ABTS, and others (Liu et al. 2016).

µPADs as a low-cost and portable platform for glucose assays was first proposed by the Whitesides group in 2007 (Martinez et al. 2007). Their device was fabricated by paper-based photo-lithography with a glucose concentration measurement range of 0 to 500 mM. Whatman® chromatography paper was the most commonly used lateral flow paper substrate (Gabriel et al. 2016, 2017; Zhu et al. 2014). Hydrophobic barriers were constructed using many techniques, such as photo-lithography, wax printing, hot embossing and screen printing (Liu et al. 2016). After, the enzymes and substrates are always

loaded onto the device manually. The limits of detection (LODs) with image data collected by a scanner or common digital camera is reported in the literature as ranging from 0.1 to 5 mM (Liu et al. 2016; Martinez et al. 2008).

Although colorimetric detection provides many advantages, it also exhibits some drawbacks that can adversely affect the analytical performance of the μPAD. The washing effect (De Tarso Garcia et al. 2014; Martinez et al. 2007; Oyola-Reynoso et al. 2015), uneven color development formed in the detection zones (Cai et al. 2014; Gabriel et al. 2017; Mohammadi et al. 2015), and enzyme/substrate loading overflow are three of the major problems. The washing effect is caused by the washing of the reagents and enzymes from the printed position to the edges of the testing zone when the sample solution travels through the patterned channels. Uneven color development and overflowing are primarily caused by unbalanced manual reagent loading and spreading of the fluid in porous cellulose fiber structure. Recent publications have achieved noticeable improvements to minimize these effects (Evans et al. 2014b; Gabriel et al. 2016; Giokas et al. 2014; Wang et al. 2012). However, the problems remained at the visual level.

In this study, we introduce a novel inkjet printing method to fabricate the paper device on Whatman® chromatography filter paper. This method overcomes the drawbacks previously described. Firstly, the nominal drop size of the nozzle is 10 pL. Generally, a 40 μm spot can be produced with a 10 pL drop. Therefore, the designed pattern could be printed out precisely because of the high printing resolution, and the spreading of liquid ink can also be minimized due to the extra low volume of each ink drop. Therefore, the overflowing and uneven color development issue can be addressed. Secondly, the application of CHI as immobilization support has been successfully demonstrated by other researchers for sensing studies (Gabriel et al. 2016; Liu et al. 2013; Vosmanská et al. 2015). Here, the CHI was printed to immobilize the enzymes (GOx and HRP) by the entrapment method (Witkowska Nery 2016) to minimize the washing effect.

In addition, the use of a cell phone is more applicable for POCTs, as smartphones are portable, have excellent computing power, and have high-resolution cameras that can quantify color intensity. An Android smartphone application was developed for the colorimetric assay of our paper-based device. The smartphone-based colorimetric measurement results were evaluated by comparing with the results from the digital scanner method.

2 Materials and methods

2.1 Materials and chemicals

Whatman® chromatography paper No.1 was purchased from GE Healthcare Life Sciences. Black cartridge-free ColorQube

ink was purchased from Xerox. Triton X-100 surfactant was purchased from MP Biomedicals, Inc. 3,3′,5,5′-tetramethylbenzidine (TMB), 2,6-dimethyl-4-heptanol, glucose oxidase from Aspergillus niger (227,533 U/g, GOx), peroxidase from horseradish (≥250 U/mg, HRP), and chitosan powder low MW were purchased from Sigma-Aldrich. Phosphate-buffered saline (PBS), was used as the solvent.

2.2 Lateral flow paper substrate

The lateral flow sensor pattern was designed using Autodesk AutoCAD software. It consists of a 6 mm square testing area and a 6 mm diameter circular dropping area connected by a 6 mm long, 4 mm wide lateral flow column. This area is surrounded by a 2 mm wide wax ink border, bringing the total size of the testing area plus ink border to a 2 mm long, 1 mm wide rectangle. The lateral flow sensor was constructed by printing the specified ink on the chromatography paper with a Xerox® ColorQube 8570 printer at a resolution of 600 DPI. The sensors were then baked on a hot plate at 150 °C for 1 min to allow the ink to penetrate the chromatography paper, creating a hydrophobic barrier.

2.3 Inks

Three liquid solutions were used in the construction of the biosensor. First, chitosan 0.2% v v^{-1} was prepared in acetic acid 0.4% v v^{-1} before fill into cartridge. TMB was dissolved in acetonitrile, then mixed acetonitrile with 2,6-dimethyl-4-heptanol at a volume ratio 1:3. The final concentration of TMB was 20 mM. The enzyme solution was prepared by adding 10 ml PBS, 20 μl Triton X-100, and 200 μl each of GOx (5 mg/ml) and HRP (1 mg/ml) to a 15 ml centrifuge tube. Both solutions were stored at 4 °C.

2.4 Sensor fabrication

2 ml of the previous solutions were added into separate 10 pl Dimatix Materials Cartridges. The paper substrate was secured in a Fujifilm Dimatix DMP-2831 printer, and the cartridge containing the 0.2% chitosan solution was loaded and printed onto the 6 mm square testing area on the assay at 40 V for two layers using 16 printing nozzles, with a 2-min delay between layers. The paper was allowed to dry for 5 min, then TMB and enzyme solution was printed onto the 6 mm square testing area at 25 V for two layers using 16 printing nozzles, with a 5-min delay between layers in order to ensure proper drying. Constructed sensors were covered and stored in a desiccator at 4 °C. the whole fabrication procedure is illustrated in Fig. 1 below.
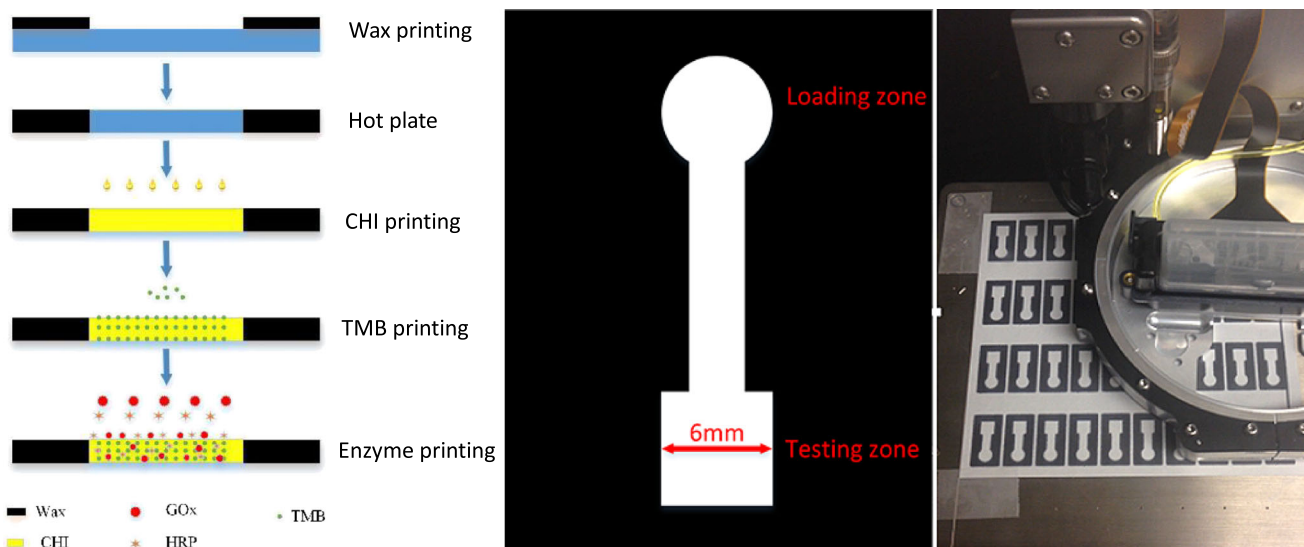
Fig. 1 The flow chart of the μPAD fabrication procedure (left), schematic diagram of device for glucose detection (middle) and the paper device printing using DMP 2831 material printer (right)

2.5 Artificial urine

The artificial urine used was prepared at pH of 6.0 according to reference (Martinez et al. 2007). The artificial urine solution was 1.1 mM lactic acid, 2.0 mm citric acid, 25 mM sodium bicarbonate, 170 mM urea, 2.5 mM calcium chloride, 90 mM sodium chloride, 2.0 mM magnesium sulfate, 10 mM sodium sulfate, 7.0 mM potassium dihydrogen phosphate, 7.0 mM dipotassium hydrogen phosphate, and 25 mM ammonium chloride all mixed in Millipore water. The pH of the solution was adjusted to 6.0 through the addition of 1.0 M hydrochloric acid. 10 ml of urine and 40 mg of glucose was added to a 15 ml centrifuge tube to create a 4 mg/ml glucose solution. This 4 mg/ml solution was then diluted to create 4 ml each of 4.0, 2.0, 1.0, 0.5, 0.25, 0.1, 0.05, 0.025 and 0.01 mg/ml glucose solutions, for a total of 9 glucose solutions ranging from 0.01 to 4 mg/ml.

2.6 Colorimetric detection

15 μl of various glucose solutions were pipetted onto the circular dropping areas of the row of seven glucose sensors. The color change was observed and recorded after 5 min of the sample loading. Colorimetric measurements were performed with an office scanner (Epson perfection V19) using 600dpi resolution. The recorded image was converted to an 8-bit grayscale image and inverted black and white by ImageJ software. Then, the arithmetic mean of the gray pixel intensity within each detection zones was used to determine the glucose concentration. The grayscale value should be positively correlated to glucose concentration.

2.7 Characterization

The morphology of the chitosan and enzyme-modified cellulose paper surface was characterized by FEI Quanta FEG 650 Scanning Electron Microscopy (SEM). Three types of samples were analyzed: an untreated control sample, a pipetted sample (chitosan and enzyme mixture pipetted onto cellulose paper manually) and a printed sample (chitosan and enzymes mixture printed onto cellulose paper by ink-jet printing). Samples were characterized under low vacuum mode at magnification of 200 times.

2.8 Smartphone application

An Android smartphone application was developed for image capture and glucose concentration measurement. The Galaxy J3V Smartphone (Android version 8.0.0), manufactured by Samsung (Suwon, Korea), was used as the application carrier. All images were captured after all camera settings were set to 'auto' and analyzed by the smartphone application, "GluMeter." The user interface and operating processes are illustrated in Fig. 2.

Button "IMAGE" is for the user to capture or load the image from the camera or from files. Button "RGB" is used to set the RGB ratio, and the grayscale value is calculated as a weighted sum of the luminance of the three color components. Button "GRAY" is to calculate and show the mean gray value of the image. Button "OVAL" is to crop the image view to an oval image view. Since the linear range is from 0.0 25 mg/ml to 0.5 mg/ml, the linear regression is for low concentration samples and the logarithmic regression is for high concentration samples. Parameters of regression equations are preset and changeable.
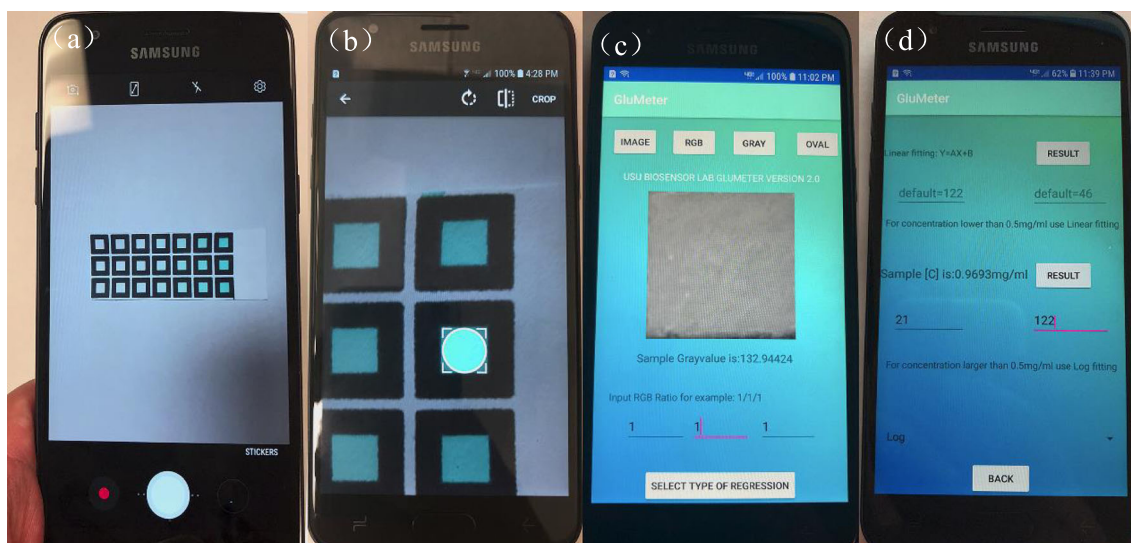
Fig. 2 The software user interface and operating process, camera image capture (**a**), crop the area of interest (**b**), input RGB ratio and calculate average gray value of the image view (**c**), select type of regression and input parameter for final concentration result

3 Results and discussion

3.1 Optimization of the ink ingredient and printing procedures

Differing from the conventional pipette dotting method, fluids (ink) should have the typical physical characteristics, including relatively high viscosity and low surface tension to optimize the inkjet printing performance. In this case, ink needs to be colorless and compatible with the enzymes. Because of its low cost and printing feasibility, chitosan(CHI) was chosen for enzyme immobilization by the entrapment method(Witkowska Nery 2016). The chitosan solution is made at 1% in 2% acetic acid and then diluted to 0.2% with DI water so that the viscosity of chitosan ink falls into the printable range. The colorimetric performance of μPADs without and with chitosan coating was illustrated in Fig. S1. The cyan color bleeding can be easily observed at the μPADs without CHI coating. TMB was chosen as the chromogenic substrate for HRP due to its non-polar molecular structure and hydrophobicity. This property prevents the dye bleeding when in contact with aqueous solvents. For TMB substrate printing, a mixture of acetonitrile (25% v/v) with 2,6-dimethyl-4-heptanol(75%v/v) provides around 5.9 cPs viscosity, suitable for printing. The solvent mixture dried in a few minutes, and the bi-enzyme solvent can then be printed. 0.2% (v/v) Triton X-100 was added to lower the surface tension of the aqueous solution. Nozzles with surface tension outside of the correct range were still usable, but with limited performance. To increase the viscosity without affecting enzymatic activity, 0.1 g/ml PEG 6000 was added to the enzyme ink. The final viscosity of the mixed solvent was 5.0 cPs. Another function of PEG 6000 was to act as an enzyme stabilizer (Novaes et al. 2014; Soares et al. 2002), helping to retain enzymatic activity at a low pH =4.0–6.0. Additional

information regarding the viscosity of the mixed solvents can be found in Table S1.

The required concentration and volumes of CHI, TMB chromogen, and bi-enzyme mixture were also optimized. The highest color intensity was achieved using a 0.2% chitosan solution and a double-layer printing at 40 V, 25 mM TMB 2 layer printing at 25 V and enzyme mixture (HRP: GOx) at 20μg/ml:100μg/ml (5 U/ml:22.75U/ml) 2 layer printing at 25 Volts. Since the drip volume for each reagent at the chosen voltage was approximately 10pL and the number of drips needed was given by the printer software, we can easily calculate the total volume for each layer of printing. The optimal enzyme mixture and substrate concentration were determined based on the result in Fig. S2. Increasing the TMB concentration or decreasing the enzyme mixture concentration caused a decrease in the color intensity. Too high of an enzyme concentration or too low of a TMB substrate concentration led to a color change from cyan/blue to brown (Fig. S2).

3.2 SEM characterization of the paper surface

The chitosan solution, TMB substrate, and enzymes were printed on Whatman® No.1 cellulose paper during the device fabrication procedure. The morphology of the modified and unmodified cellulose paper surface was characterized by an FEI Quanta FEG 650 scanning electron microscope (SEM). Based on the results presented in Fig. 3, it is possible to observe the surface morphology differences between the modified groups and control group. The porous structure of cellulose on printed and pipetted samples was partially coated by a mixture of chitosan and enzymes in the form of a thin film. Theoretically, the printed layer of chitosan and enzyme thin film layer should have better coating uniformity. However, there was no significant difference that can be visually
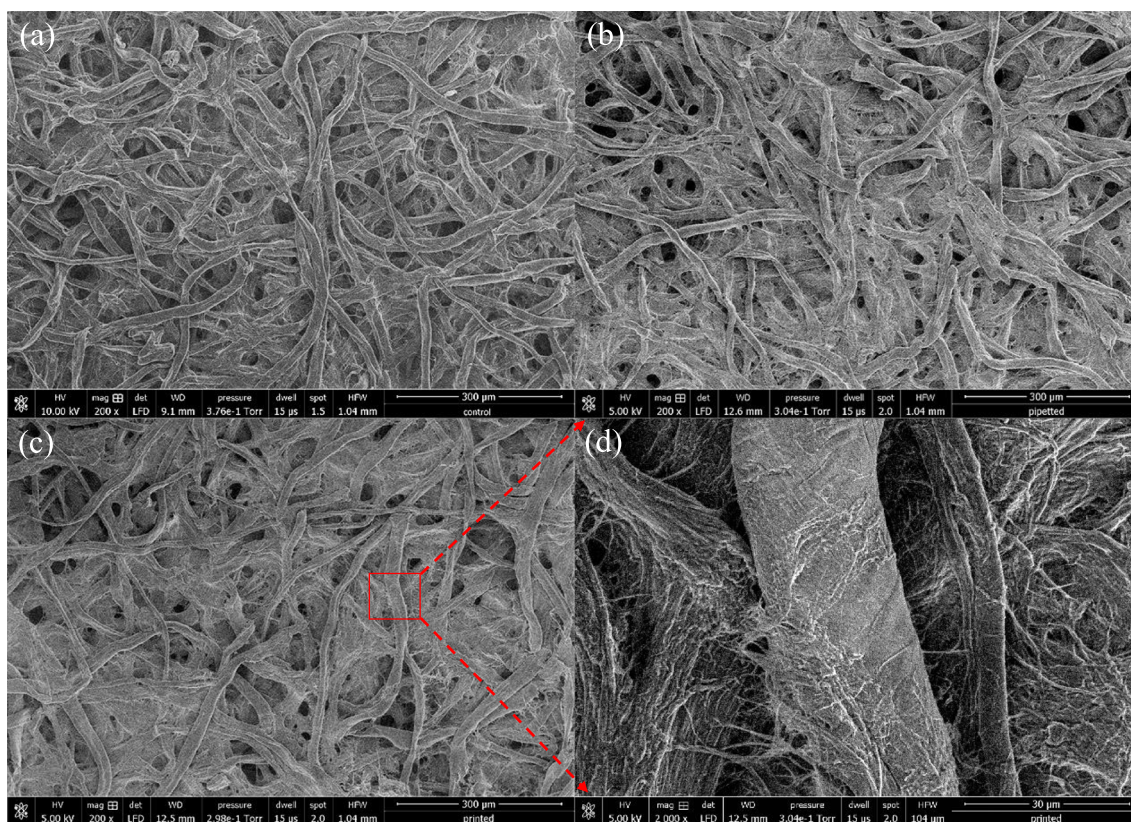
Fig. 3 The SEM images showing the morphology of the cellulose paper surface, nature cellulose paper (**a**), CHI and protein pipette coating (**b**) CHI and protein printing coating (**c**), and 2000× magnification at red square highlighted area (**d**). Scale bars: 300 μm (a-c), 30 μm (d)

observed in Fig. 3b, c between the printed and pipetted samples. The size of cellulose fiber ranged from several μm to tens of μm (Fig. 3d).

3.3 Analytical curve

For calibration of the biosensor, one drop (15 ml) of artificial urine (0–4 mg/mL (22 mM)) was added onto the loading zone of a μPAD, and the liquid was allowed to spread and travel throughout the whole zone by capillary action. Once the reaction was complete (5 min), the paper was scanned using an office scanner and the image was saved. The images were then analyzed by ImageJ to obtain the grayscale value for each sensing zone.

According to optical graphs presented in Fig. 4, the visual detection associated with the increment on the characteristic cyan color of TMB substrate in the detection zones corresponds to all tested glucose concentrations. As we can see, the cyan color in the sensing zone was uniformly distributed without washing effect and overflowing of color. Compared with previously published results, our current method was straightforward, low cost, and without the need of special treatment of the substrate such as oxidation (De Tarso Garcia et al. 2014), incorporation of functionalized nanoparticles (Evans et al. 2014b; Figueredo et al.

2015) or flow control (Giokas et al. 2014). Additionally, the result also indicated uniformly printed layers with the appropriate mixture of CHI, TMB substrate, and enzymes. In order to show the repeatability of our method, the experiment was repeated for 5 times. The complete results can be found in Fig. S3.

The analytical performance of the printed μPADs was evaluated. According to the analytical curves illustrated in Fig. 5, the intensity of the cyan color is proportional to glucose concentration. The assay displayed a linear profile from 0.0 25 mg/ml to 0 .5mg/ml with correlation coefficient values at 0.996, but non-linear profile from overall scale 0.01 mg/ml to 4 mg/ml. The data were then linearized by comparing the mean color intensity and the logarithm of the glucose concentration. The correlation coefficient value (R^2) was 0.965.

The limit of detection (LOD) for each bioassay was calculated based on the mean of the blank (Mean (Blank)) and the standard deviation for the blank (SD) ($n = 25$). The formula was LOD = Mean (blank) + 3SD. The LOD values achieved for glucose were 0.01 01 mg/ml (0.0 56 mM),

The cost of inks and paper substrate has been estimated to be $30 USD in total and it has allowed the fabrication of more than 1000 μPADs with great reproducibility and long shelf life. The final unit cost of the μPAD was approximately
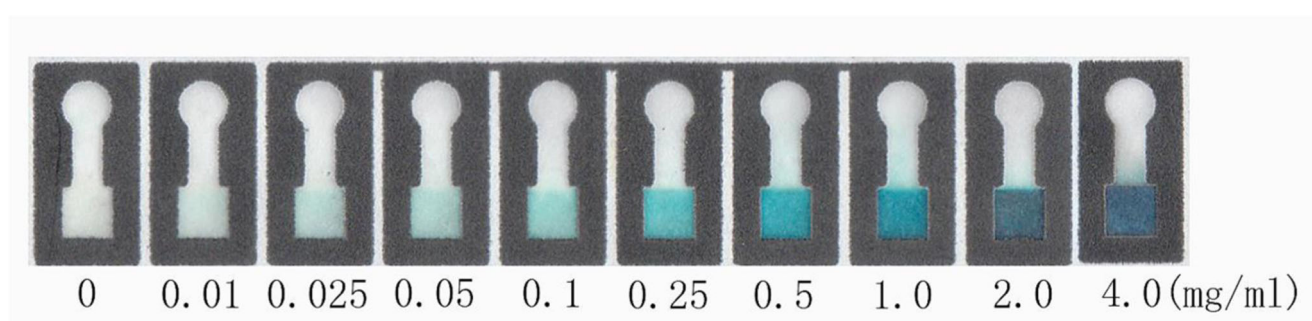
Fig. 4 Images of the printed μPAD corresponding to glucose assays in concentrations ranging from 0 to 4 .0mg/ml

$0.06 USD. Currently, the unit price of commercially available glucose colorimetric test strips ranges from $0.17 up to $1.00 USD or higher.

In this study, we used wax and inkjet printing to fabricate the device. We then used a scanner and ImageJ to collect and analyze data. With this system, errors were mainly caused by the wetting condition of the filter paper, printer nozzle condition and printing alignment. Based on our observation, wetting increased background grayscale intensity, more wetted filter paper provided a higher background grayscale value, and less wetted paper led to a lower grayscale value. Since the wetting condition at each sensing zone and loading zone are similar, the error may be minimized by using the formula: True gray value = Gray value at sensing zone − Gray value at loading zone. The nozzles of the inkjet material printer can become blocked after many uses. Because of this, the total printing volume may be affected if nozzles become partially blocked. Theoretically, the entire sensing zones were analyzed to collect grayscale image data. However, due to imperfect alignment during printing, a small proportion of the sensing zone may not be printed and may influence the data acquisition after reactions.

3.4 Shelf life testing

The device shelf life was tested for a 60-day period with five different glucose concentrations (0.05, 0.1, 0.25, 0.5 and 1 (mg/ml)). The results are illustrated in Fig. 6 and Fig. S5 for graphic results. Based on the results, in the first 3 days, the enzymatic activity decreased to 77.8%, 90.1%, 88.7%, 83.7% and 83.8% of the tested intensity at day 1 for glucose concentration 0.05 mg/ml, 0 .1mg/ml, 0.25 mg/ml, 0 .5mg/ml and 1 mg/ml respectively. After day 3, the colorimetric intensity of all tested concentration remained stable until 2-months after printing. The change of pH and salts concentration during the solvent volatilization in the first 3 days could be a significant cause of the loss of enzymatic activity.

PEG addition was reported as an efficient method to preserve enzymatic activities of several typical enzymes (Novaes et al. 2014; Soares et al. 2002; Talukder et al. 2003). For our case, the μPADs with PEG6000 added in the ink has contributed to a higher color intensity at the same level of glucose concentration (Fig. S4). Moreover, without adding PEG6000, the enzymes lost most of their function in less than 3 days (Fig. S4).
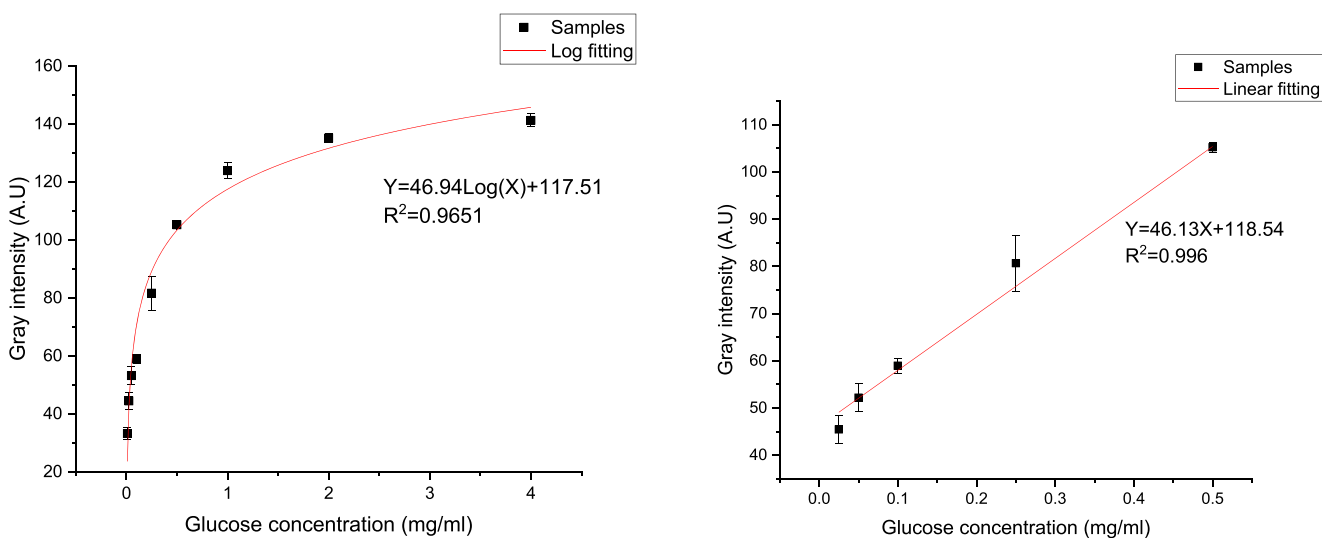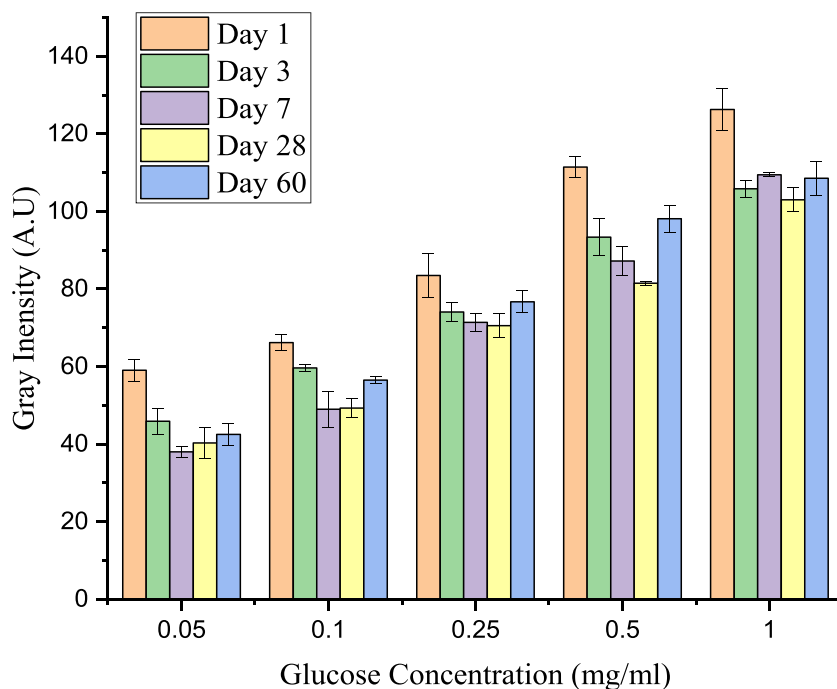

Fig. 5 Analytical curves for glucose, $(Y = 46.94 \log(X) + 117.51$, $R^2 = 0.965)$ assays performed on μPADs ($n = 5$) (left) and linear ranges $(Y = 46.13X + 118.54$ $R^2 = 0.996)$ of the analytical curve for glucose using inkjet printed μPAD (right)

Fig. 6 Shelf life testing of μPAD
with different glucose
concentrations for maximum
60 days (*n* = 3)

3.5 Recovery experiments

The accuracy of the μPAD devices was evaluated
through recovery experiments. The recovery test was
conducted by adding artificial urine with a standard glu-
cose concentration (0.15 mg/ml, 0.75 mg/ml and
1 .5mg/ml). As can be seen in the presented data in
Table 1, the μPADs recovery values varied between
102.8% and 110.1%. 10 replicate measurements were ar-
chived for each concentration (*n* = 10) and the more de-
tailed graphs were demonstrated in Fig. S6. Due to the
standardized device fabrication procedures, the standard
deviation was smaller than that of previously published
results (Figueredo et al. 2015; Gabriel et al. 2016, 2017;
Oyola-Reynoso et al. 2015), and the error values were
similar regardless of the sample glucose concentration.
Since the standard deviation was a nearly fixed value in
our case, the RSD increased while testing samples with
lower glucose concentration.

Table 1 Glucose concentration levels determined with artificial urine
samples using inkjet printed μPADs

| Known concentration (mg/ml)	Measured concentration (mg/ml)	RSD (%)	Recovery (%)
0.150	0.161 ± 0.019	11.9%	107.3%
0.750	0.771 ± 0.021	2.8%	102.8%
1.500	1.651 ± 0.022	1.3%	110.1%

Recovery test was conducted by adding three different concentrations of
standard solution (*n* = 10) RSD: Relative standard deviation

3.6 Compare smartphone-based method with the scanning method

An Android smartphone application was developed to capture
the image, process data, and calculate the glucose concentra-
tion. Here we compared the colorimetric test results from both
the smartphone-based method and scanning method followed
by ImageJ data processing. Five different glucose concentra-
tions (0.05, 0.1, 0.25, 0.5 and 1 mg/ml) were used for this
assay. For the smartphone-based method, the images captured
were from both indoor and outdoor environments.

The regression equations and R-Squares values of all
methods were illustrated in Fig. 7. As we can see, the
scanner method had the best R-square value (R^2 =
0.9979), because the lighting conditions were the same
at all locations during scanning. The standard deviations
of the smartphone-based method were much larger than
the scanner method. Possible reasons could be the varia-
tion of the angle and distance between external light
sources and the paper surface during the image capture.
More importantly, the major difference of grayscale value
at the same concentration point was caused by the vari-
ance of ambient light intensity in different environments.
The scanner supplied the highest brightness and hence
produced the lowest inverted grayscale value in the curve.
Given the complication of the ambient light source, re-
calibration is needed if the location is changed while
using the smartphone-based method. Providing consistent
illumination would significantly improve the performance
of this method. Another major challenge of using a
smartphone for colorimetric readout is the variation of

Fig. 7 Paper-based device image result collected with different methods(top), and glucose analytical curves of different methods (All methods were using the same sample paper)
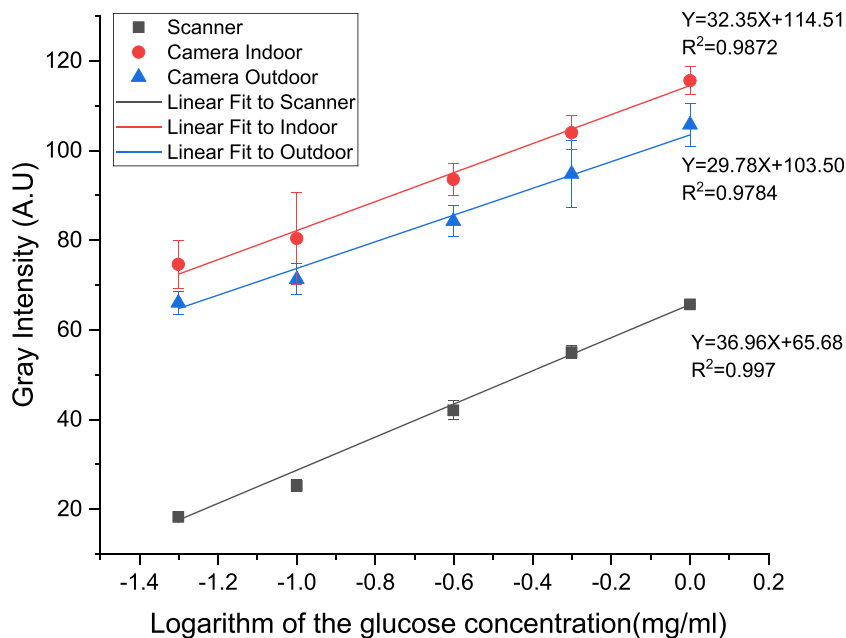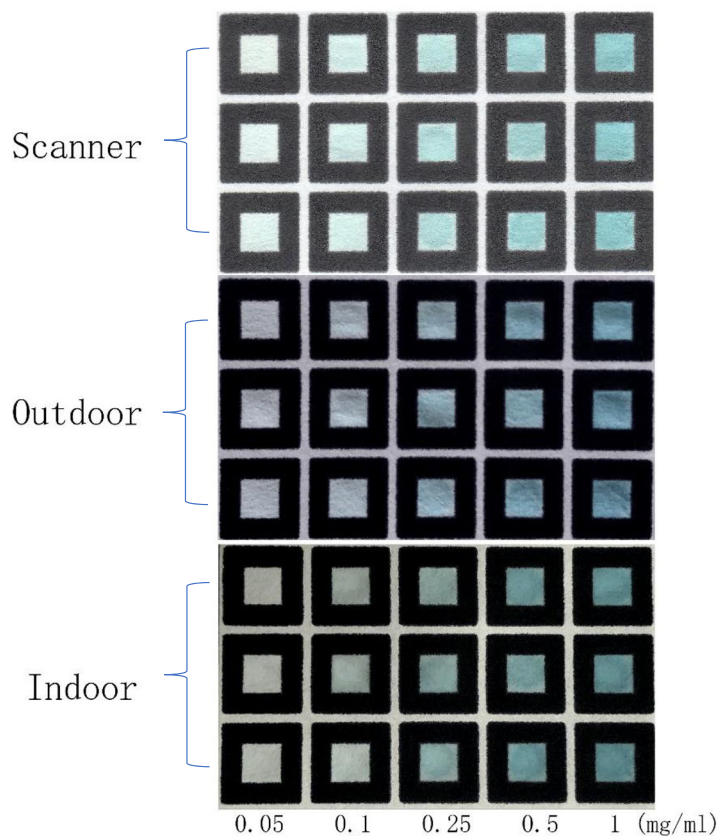
the image capture parameters on different brands of smartphones while using a build-in auto camera. Parameters such as exposure time, light sensitivity and white balance would significantly affect the signal baseline of images. In order to minimize these effects, our smartphone application was developed with the ability to manually set and fix these parameters at a certain value during the image capture.

Fig. 8 Comparison of the unknown glucose concentrations in artificial urine samples determined by μPAD (*n* = 5) and spectrophotometer (*n* = 3)

Samples with unknown glucose concentration
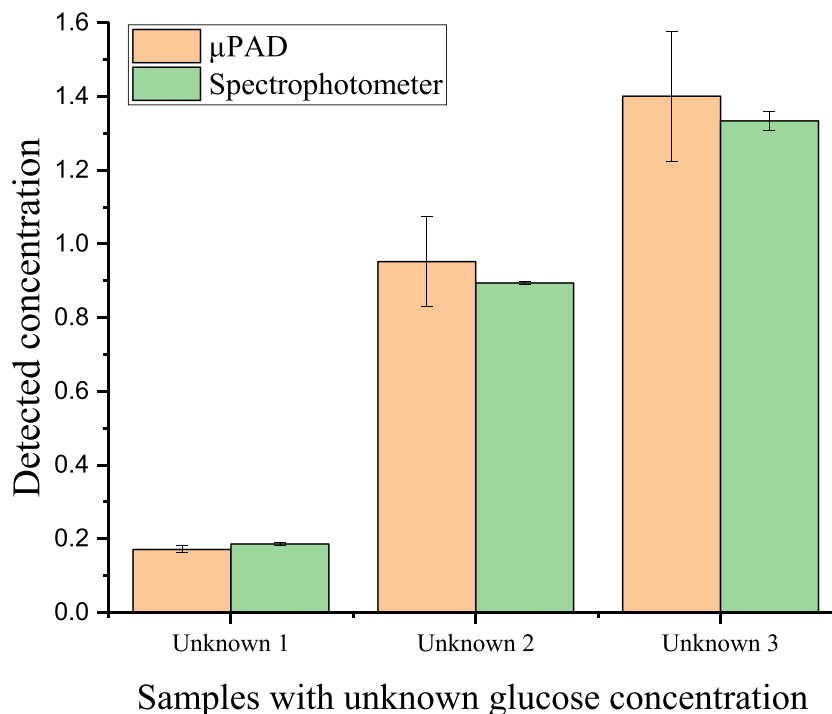
3.7 Comparison with the reference method

Spectrophotometry was chosen as the reference method. The Glucose (HK) assay kit was purchased from Sigma-Aldrich®, and the ultraviolet absorbance at a wavelength of 340 nm was directly proportional to the sample glucose concentration. Three artificial urine samples with unknown glucose concentration were prepared and tested. The measurement results (Fig. 8) by both μPAD (Fig. S7) and reference method (Spectrophotometer) were statistically compared, the *P* values of one-way ANOVA were calculated and ranged from 0.085 to 0.504. From this, it can be concluded the data collected from both methodologies were not statistically different from one another at a confidence level of 95%.

4 Conclusion

In summary, an inkjet-printed paper-based colorimetric biosensor was developed for urine glucose monitoring at the point-of-care. The device was first wax printed to form a hydrophobic barrier. Then, CHI, enzymes, and TMB were inkjet-printed onto the testing zone. The surface CHI and enzyme coating was evaluated by SEM. The approach was successfully applied to quantify glucose in the clinically relevant range from 0.01 mg/ml (55 nM) to 4 mg/ml (22 mM). The limit of detection was 0.01 mg/ml (56 μM). This standardized printing method reduced the cost of each testing unit, minimized the washing effect, and improved the uniformity, accuracy and repeatability. The addition of PEG6000 provided a long shelf life and

enhanced analytical performance, allowing the visual detection of glucose at low concentrations. The device retained over 80% percent enzymatic activity after 2-month storage at 4 °C. The smartphone-based colorimetric imaging method was evaluated and the disadvantages associated with differing external light sources could be solved by providing consistent illumination. The proposed device is portable, low-cost and easy to use, providing great potential to be applied in point-of-care testing in the developing world. Furthermore, this printing method is applicable to any other enzyme/substrate system.

References

L. Cai, Y. Wang, Y. Wu, C. Xu, M. Zhong, H. Lai, J. Huang, Analyst. **139**, 4593 (2014)

P. De Tarso Garcia, T.M. Garcia Cardoso, C.D. Garcia, E. Carrilho, W.K. Tomazelli Coltro, RSC Adv. **4**, 37637 (2014)

W. Dungchai, O. Chailapakul, C.S. Henry, Anal. Chem. **81**, 5821 (2009)

E. Evans, E.F. Gabriel, T.E. Benavidez, W.K. Tomazelli Coltro, C.D. Garcia, Analyst. **139**, 5560 (2014a)

E. Evans, E.F.M. Gabriel, W.K.T. Coltro, C.D. Garcia, Analyst. **139**, 2127 (2014b)

F. Figueredo, P.T. Garcia, E. Cortón, W.K.T. Coltro, ACS Appl. Mater. Interfaces **8**, 11 (2015)

E.F. Gabriel, P.T. Garcia, T.M. Cardoso, F.M. Lopes, F.T. Martins, W.K. Coltro, Analyst. **141**, 4749 (2016)

E. Gabriel, P. Garcia, F. Lopes, W. Coltro, Micromachines. **8**, 104 (2017)

D.L. Giokas, G.Z. Tsogas, A.G. Vlessidis, Anal. Chem. **86**, 6202 (2014)

J. Hu, S. Wang, L. Wang, F. Li, B. Pingguan-Murphy, T.J. Lu, F. Xu, Biosens. Bioelectron. **54**, 585 (2014)

C.H. Lee, L. Tian, S. Singamaneni, ACS Appl. Mater. Interfaces **2**, 3429 (2010)

B. Li, W. Zhang, L. Chen, B. Lin, Electrophoresis. **34**, 2162 (2013)

W. Li, D. Qian, Q. Wang, Y. Li, N. Bao, H. Gu, C. Yu, Sens. Actuators. B. Chem. **231**, 230 (2016)

H. Liu, R.M. Crooks, J. Am. Chem. Soc. **133**, 17564 (2011)

W. Liu, C.L. Cassano, X. Xu, Z.H. Fan, Anal. Chem. **85**, 10270 (2013)

S. Liu, W. Su, X. Ding, Sensors., **16** (2016)

A. Määttänen, U. Vanamo, P. Ihalainen, P. Pulkkinen, H. Tenhu, J. Bobacka, J. Peltonen, Sens. Actuators. B. Chem. **177**, 153 (2013)

A.W. Martinez, S.T. Phillips, M.J. Butte, G.M. Whitesides, Angew. Chem. **46**, 1318 (2007)

A.W. Martinez, S.T. Phillips, E. Carrilho, S.W. Thomas Iii, H. Sindi, G.M. Whitesides, Anal. Chem. vol 80 (2008), p. 3699

A. W. Martinez, S. T. Phillips, G. M. Whitesides and E. Carrilho, Diagnostics for the developing world: microfluidic paper-based analytical devices. ed.)^eds.), ACS Publications (2009)

S. Mohammadi, M. Maeki, R.M. Mohamadi, A. Ishida, H. Tani, M. Tokeshi, Analyst. **140**, 6493 (2015)

L.C.D.L. Novaes, A.F. Jozala, P.G. Mazzola, A.P. Júnior, Braz. J. Pharm. Sci. **50**, 371 (2014)

S. Oyola-Reynoso, A.P. Heim, J. Halbertsma-Black, C. Zhao, I.D. Tevis, S. Cinar, R. Cademartiri, X. Liu, J.F. Bloch, M.M. Thuo, Talanta. **144**, 289 (2015)

L. Shen, J.A. Hagen, I. Papautsky, Lab Chip **12**, 4240 (2012)

A.L. Soares, G.M. Guimaraes, B. Polakiewicz, R.N. De Moraes Pitombo, J. Abrahao-Neto, Int. J. Pharm. **237**, 163 (2002)

M. Talukder, T. Takeyama, Y. Hayashi, J. Wu, T. Kawanishi, N. Shimizu, C. Ogino, Appl. Biochem. Biotechnol. **110**, 101 (2003)

N.K. Thom, G.G. Lewis, K. Yeung, S.T. Phillips, RSC Adv. **4**, 1334 (2014)

S.K. Vashist, O. Mudanyali, E.M. Schneider, R. Zengerle, A. Ozcan, Anal. Bioanal. Chem. **406**, 3263 (2014)

V. Vosmanská, K. Kolářová, S. Rimpelová, Z. Kolská, V. Švorčík, RSC Adv. **5**, 17690 (2015)

S. Wang, L. Ge, X. Song, J. Yu, S. Ge, J. Huang, F. Zeng, Biosens. Bioelectron. **31**, 212 (2012)

W.Y. Wei, I.M. White, Analyst. **138**, 1020 (2013)

X. Wei, T. Tian, S. Jia, Z. Zhu, Y. Ma, J. Sun, Z. Lin, C.J. Yang, Anal. Chem. **88**, 2345 (2016)

E. Witkowska Nery, Analysis of glucose, cholesterol and uric acid. In Analysis of Samples of Clinical and Alimentary Interest with Paper-Based Devices. pp. 25, (2016)

M. Zhou, M. Yang, F. Zhou, Biosens. Bioelectron. **55**, 39 (2014)

W.-J. Zhu, D.-Q. Feng, M. Chen, Z.-D. Chen, R. Zhu, H.-L. Fang, W. Wang, Sens. Actuators. B. Chem. **190**, 414 (2014)